PHYSICAL REVIEW E **81**, 041904 (2010)

Puff-wave transition in an inhomogeneous model for calcium signals

J. W. Shuai,[1,*] Y. D. Huang,[1] and S. Rüdiger[2]
[1]*Department of Physics and Institute of Theoretical Physics and Astrophysics, Xiamen University, Xiamen, Fujian 361005, China*
[2]*Institute of Physics, Humboldt University Berlin, Newtonstr. 15, 12489 Berlin, Germany*
(Received 21 September 2009; revised manuscript received 17 February 2010; published 6 April 2010)

In many cell types, calcium ion channels on the endoplasmic reticulum membrane occur in a clustered distribution. The channels generate either localized puffs, each comprising channels of only one cluster, or global calcium waves. In this work we model the calcium system as a two-dimensional lattice of active elements distributed regularly in an otherwise passive space. We address an important feature of the puff-wave transition, which is the difference in lifetime of puffs at a few hundred milliseconds and long-lived global waves with periods of several seconds. We show that such a lifetime difference between puffs and waves can be understood with strongly reduced ordinary differential equations modified by a time-scale factor that takes into account the coupling strength of active and passive regions determined by the Ca^{2+} diffusion coefficient. Furthermore, we show that the point model can also describe very well the dependence of Ca^{2+} oscillation characteristics on the cluster-cluster distance in the case of large diffusivity.

DOI: 10.1103/PhysRevE.81.041904 PACS number(s): 87.16.Xa, 87.18.Hf, 87.16.Vy, 82.20.Uv

I. INTRODUCTION

Since the discovery of calcium release puffs and their association with clusters of inositol 1,4,5-trisphosphate (IP_3) receptor (IP_3R) channels on the endoplasmic reticulum (ER) membrane, clustering has emerged as a defining feature of intracellular calcium signals [1–3]. With a clustered distribution of IP_3Rs, calcium signals are either global waves, which modulate cellular behavior, or localized puffs, which control subcellular processes [4]. In experiments, puffs occur at small levels of release-stimulating second messenger IP_3, whereas waves appear at large IP_3 concentration [5]. Furthermore, puffs can also be elicited by addition of exogenous calcium buffer such as ethylene glycol tetraacetic acid (EGTA), which is believed to reduce the coupling between clusters by binding of calcium to EGTA [6,7].

The random appearance of puffs indicates a strong stochasticity of channel dynamics [5], which is caused by the low copy number of channels within each cluster [8]. Much recent work focused on the stochastic dynamics of individual IP_3R clusters [8–14] and the functional significance of clusters. Among these studies, Shuai and Jung showed that there is a dependence of the frequency of puff signals on the actual channel number in a cluster and thus that the calcium system may use the clustered IP_3Rs to achieve an optimal puff signaling [9].

An important question is how exactly the more deterministically appearing global waves and strongly stochastic localized events can be generated by the same system apparently upon variation of only a few of the system's parameters. In theoretical studies, the hierarchical organization of channels and clusters, combined with the complex and stochastic IP_3R kinetics, supports a variety of spatiotemporal patterns of calcium release [15–21]. It has been shown that clustered IP_3R distributions with stochastic channel dynamics can enhance the cell's Ca^{2+} sensitivity responding to weak IP_3 stimulus [15]. Falcke extended the emerging concept of stochastic calcium release to general intracellular calcium oscillations and thus placed the system into the realm of stochastically forced excitable systems [17]. The random nature of calcium signaling is, from this point of view, a consequence of the stochasticity of channel clusters and expresses itself at a higher level in fluctuations of attributes of global calcium oscillations [19].

The clustering not only causes a strong stochasticity of local calcium release but it also generates a spatially inhomogeneous reaction-diffusion medium. The inhomogeneity caused by the clustering of channel has already been addressed by considering purely deterministic pattern formation. It has been suggested that a reaction-diffusion system with a regular array of point source release sites can be described by a fire-diffuse-fire model [22]. It has also been found that waves in three-dimensional reaction-diffusion system with spatially confined excitability undergo propagation failure with *increasing* diffusion coefficient and that there is a regime in which the wave velocity is independent of the diffusion coefficient [23]. This study indicates that waves in inhomogeneous media can have counterintuitive properties that do not appear in homogeneous system.

In the present work we aim to discuss the lifetime difference between puff and wave of Ca^{2+} signals with a simple deterministic two-dimensional (2D) model with a regular lattice of active elements distributed in a passive space. In our model the coupling of channels within the cluster occurs through the calcium concentration of the cluster, while the coupling of channels in different clusters occurs through the diffusion of the activating agent, i.e., calcium, through the passive space between clusters. With respect to the puff-wave transition, we will thus in this paper describe a noticeable feature of Ca^{2+} signals, i.e., the transition from synchronized long-lived oscillations (waves) to desynchronized short-lived activity (puffs) of individual elements upon addition of EGTA buffer. Following the earlier consideration of Dargan and Parker we attribute the apparent reduction of synchronization by EGTA to the lowering of effective cal-

*Corresponding author. FAX: (86) 592-218-9426; jianweishuai@xmu.edu.cn

cium mobility between clusters and study the dynamical behavior of a reduced model for changing diffusion coefficient. We show that the different lifetimes of puff and wave of Ca^{2+} signal can be understood with a strongly reduced ordinary differential equation modified by a time-scale factor that takes into account the coupling strength of active and passive regions determined by the Ca^{2+} diffusion coefficient. Furthermore, the point model can also describe very well the dependence of Ca^{2+} oscillation characteristics on the cluster-cluster distance in the case of large diffusivity.

II. METHODS

A. Cytosolic Ca^{2+} diffusion

In our model, intracellular calcium dynamics are described by a reaction-diffusion approach with calcium release regions discretely distributed on a two-dimensional ER membrane. The equation for Ca^{2+} ions ($[Ca^{2+}]$) with diffusion coefficient D is given as follows:

$$\frac{\partial[Ca^{2+}]}{\partial t} = D\nabla^2[Ca^{2+}] + f(x,y) \times J_{\text{cluster}}. \tag{1}$$

The diffusion constant in the cytoplasm D includes mobile and immobile bufferings and should be regarded as an effective diffusion constant. EGTA, for instance, takes up calcium ions at the active cluster and diffuses with its own mobility through the medium. Since the diffusion coefficient of EGTA is smaller than that of calcium, addition of EGTA thus reduces the effective diffusion coefficient of calcium. The approximations for the buffer dynamics, such as the rapid buffer approximation, motivate this simplified handling of EGTA [24]. Although EGTA is not a rapid buffer, it should be noted that nevertheless a reduction of effective mobility of calcium can be expected. Owing to the large spatial separation of clusters, calcium can bind to EGTA well before it reaches adjacent clusters, which slows down the motion of calcium through the cytosol. Thus, for sufficient amounts of buffer, one obtains a reduction of the effective diffusion coefficient.

We represent the ER membrane as a mosaic of active and passive patches. In detail, the domain is a regular array of active regions separated by regions of passive diffusion. Thus the function $f(x,y)$ in Eq. (1) is defined as

$$f(x,y) = \sum_i \sum_j \left[\Theta\left(x - iL - \frac{l}{2}\right) - \Theta\left(x - iL + \frac{l}{2}\right)\right] \times \left[\Theta\left(y - jL - \frac{l}{2}\right) - \Theta\left(y - jL + \frac{l}{2}\right)\right] \tag{2}$$

with the Heaviside function $\Theta(x)=0$ for $x<0$, otherwise 1. As a result, the function $f(x,y)=1$ at the active patches, otherwise, $f(x,y)=0$. Each active region is a square with a side length of l and the most nearby active regions have a distance of L.

Three calcium fluxes are present in the active regions, i.e.,

$$J_{\text{cluster}} = J_{\text{channel}} - J_{\text{pump}} + J_{\text{leakage}}, \tag{3}$$

in which the channel flux J_{channel} describes calcium released from the ER to the intracellular space through IP_3R channels, the pump flux J_{pump} describes calcium uptake from the intracellular space back into the ER by adenosine triphosphate dependent pump with

$$J_{\text{pump}} = v_P \frac{[Ca^{2+}]^2}{k^2 + [Ca^{2+}]^2}, \tag{4}$$

and the leakage flux J_{leakage} describes the leaking flux from the ER to the intracellular space with

$$J_{\text{leakage}} = v_L([Ca^{2+}]_{\text{ER}} - [Ca^{2+}]), \tag{5}$$

where $[Ca^{2+}]_{\text{ER}}$ describes the high concentration of Ca^{2+} in ER. The parameters v_P and v_L describe the maximum pump flux and leakage rate, respectively.

B. IP_3R channel dynamics

A theoretical model for agonist-induced $[Ca^{2+}]$ oscillations based on microscopic kinetics of IP_3 and $[Ca^{2+}]$ gating of the IP_3R was proposed by De Young and Keizer [25]. The model assumes that there are three equivalent and independent subunits involved in the conduction of an IP_3R. Each subunit has one IP_3 binding site (m gate) and two Ca^{2+} binding sites, one for activation (n gate) and the other for inhibition (h gate). A simplified version of the model was proposed by Li and Rinzel [26], in which the binding probabilities of IP_3 to the m gate and activating Ca^{2+} to the n gate are instantaneous and represented by their quasi-steady-states m_∞ and n_∞.

In this paper we consider a modified Li-Rinzel model with channel flux given by

$$J_{\text{channel}} = v_C m_\infty^3 n_\infty^3 h^3([Ca^{2+}]_{\text{ER}} - [Ca^{2+}]) \tag{6}$$

with

$$m_\infty = \frac{[IP_3]}{[IP_3] + d_m},$$

$$n_\infty = \frac{[Ca^{2+}]}{[Ca^{2+}] + d_n}. \tag{7}$$

The Ca^{2+} inactivation (h gate) is slow and described by the binding and dissociation rates α and β given by

$$\frac{dh}{dt} = \alpha(1-h) - \beta h \tag{8}$$

with

$$\alpha = a_1 \frac{[IP_3] + d_1}{[IP_3] + d_2},$$

$$\beta = a_2[Ca^{2+}]. \tag{9}$$

In order to incorporate the stochasticity of channel opening or closing we use a Langevin approach,

$$\frac{dh}{dt} = \alpha(1-h) - \beta h + G(t), \tag{10}$$

where $G(t)$ is zero mean, uncorrelated, Gaussian white noise term with

TABLE I. Parameter values used in the model.

Parameter	Value
L	0.5–5.5 μm
$l(=\Delta x)$	0.25 μm
D	0.1–300 $\mu m^2/s$
$[IP_3]$	1 μM
$[Ca^{2+}]_{ER}$	12 μM
v_C	100 s^{-1}
v_P	100 $\mu M/s$
v_L	0.04 s^{-1}
d_m	0.11 μM
d_n	0.08 μM
d_1	0.17 μM
d_2	1.8 μM
a_1	0.8 s^{-1}
a_2	1.2 $(\mu M\ s)^{-1}$
k	0.1 μM

$$\langle G(t)G(t')\rangle = \frac{\alpha(1-h)+\beta h}{N}\delta(t-t'). \tag{11}$$

The stochastic channel dynamics is due to stochastic binding and unbinding processes of Ca^{2+} ions and IP_3 messengers to channels. The random initiation of puffs mainly results from the stochastic activation binding of Ca^{2+} and IP_3 to open a channel and furthermore to trigger a puff release. Here with the Li-Rinzel model the Ca^{2+} and IP_3 activation processes are eliminated and represented by their quasi-steady-state values. Therefore, the stochasticity is imposed only on the inactivation process, which for simplicity represents the randomness of puff dynamics.

C. Model parameters

The parameter values used in the model are given in Table I. Consistent with experimental data, we choose $l=0.25$ μm and L is about a few micrometers to define the active and passive regions on ER membrane. In the numerical simulation, the ER membrane is spatially discretized and represented by a two-dimensional lattice with grid distance Δx. In order to avoid a grid size Δx, which is too small in comparison to the active size l, we apply $\Delta x=l$ in our simulation for simplicity, i.e., the grid size equals the actual size of the active sites. With this approach, we assume that the calcium concentration in each cluster is always homogeneous. The cell size is fixed at 50×50 μm^2.

For this study, we assume that the concentration of Ca^{2+} in the ER remains unchanged everywhere and is thus chosen to be constant. Experiments showed that, because of the steep dependence of activation of channels on IP_3 concentration, puffs could be observed only over a narrow range of IP_3 concentrations [3,5]. A certain threshold IP_3 concentration was required to evoke any calcium release, whereas concentrations less than twice as great would evoke propagating Ca^{2+} waves. To circumvent this problem, later experiments were done by imaging Ca^{2+} signals in cells with the Ca^{2+} buffer EGTA loaded [27]. Thus even at high IP_3 concentration one can observe individual puffs with enough EGTA present, while Ca^{2+} waves will be obtained if no EGTA is added [27]. Throughout this paper, we set $[IP_3]=1.0$ μM at which the Li-Rinzel point model is an oscillatory system, and we discuss the puff-wave transition by varying the diffusion coefficients.

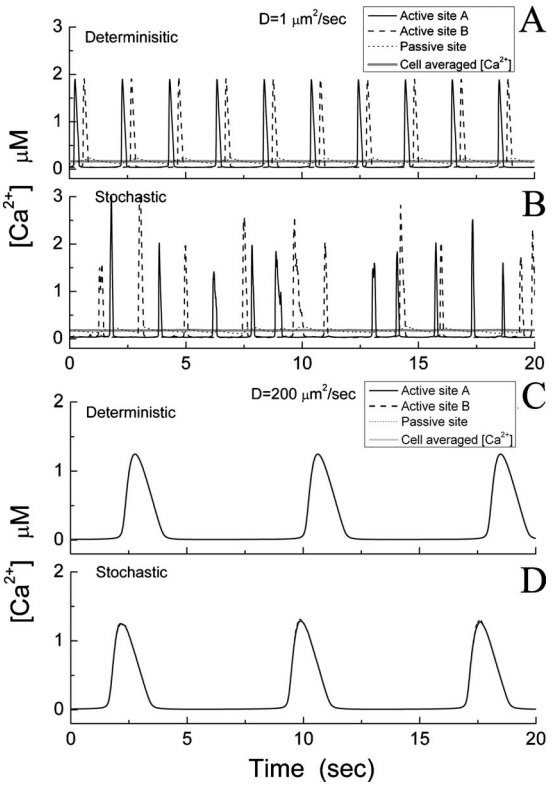

FIG. 1. The Ca^{2+} signals versus time (A) and (B) at $D=1$ $\mu m^2/s$ and (C) and (D) at $D=200$ $\mu m^2/s$. The channel dynamics are deterministic in (A) and (C) and stochastic in (B) and (D). The black line and dashed line plot the Ca^{2+} signals at two nearby active regions, the dotted line shows the Ca^{2+} signal at the passive region in the middle of the two active regions, and the gray line is the cell-averaged Ca^{2+} signal. Here $L=2$ μm.

III. RESULTS

A. Ca^{2+} puff

At small diffusion coefficient, each active region is weakly coupled to the others, generating local calcium release, i.e., Ca^{2+} puffs. Figure 1(A) shows the evolution of calcium concentration at two nearby clusters in the center of the cell model with $D=1$ $\mu m^2/s$ and $L=2$ μm. In this simulation, the channel dynamics are deterministic and described by Eq. (8). With randomized initial conditions, phase differences arise among puffs at different cluster sites. In this example, the puff period, i.e., the interpuff interval, is 2.04 s and the puff lifetime, i.e., the full width at half-maximal amplitude, is 0.136 s.

Since the IP_3R channel number in each cluster is about a few tens [10,28], the channel behavior is typically stochastic,

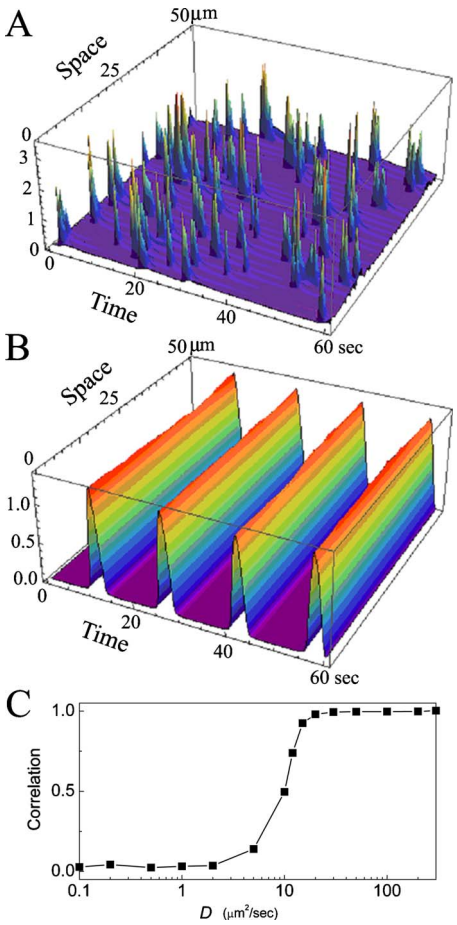

FIG. 2. (Color online) The line scan space-time imaging of (A) stochastic puffs at $D=1\ \mu m^2/s$ and (B) the stochastic waves at $D=200\ \mu m^2/s$ and $L=2\ \mu m$. The scan line crosses the center cluster. (C) The maximal cross correlation between calcium concentrations at the center cluster and its nearby cluster as a function of D.

resulting in noisy puffs. In our stochastic simulations, we assume that there are $N=25$ channels in each cluster. The stochastic channels are modeled with the Langevin approach [Eq. (10)]. Figure 1(B) shows the random appearance of puffs for the same sites as in Fig. 1(A). The mean lifetime of stochastic puffs is 1.93 s, which is close to 2.04 s for deterministic puffs. To visualize the stochastic puff patterns we show in Fig. 2(A) a space-time plot, resembling the experimental line scan images [5]. Here the visualized line crosses the center cluster. The randomness of puff release can be seen clearly in this plot.

For comparison, the calcium concentration at the middle point between these two clusters, which is inside the passive diffusion region, and the cell-averaged calcium concentration are also given. The typically small calcium concentration between the two clusters, which is quite close to the cell-averaged calcium concentration, indicates that clusters are weakly coupled. In order to discuss the coupling strength quantitatively, the cross correlation between calcium concentrations at the center cluster and its nearby cluster has been calculated as a function of time lag. Considering the possibility of synchronization with phase delay, the maximal cross correlation is typically found at a nonzero time lag. For this example, the maximal cross correlation is about 0.03 [Fig. 2(C)], indicating a weak coupling among clusters.

B. Ca^{2+} wave

Ca^{2+} waves are observed at large diffusion coefficient. Figure 1(C) shows the evolution of calcium concentration at the same sites used in Fig. 1(A) at $D=200\ \mu m^2/s$ with deterministic channel dynamics. Due to the strong coupling, the calcium concentrations at both the active sites and passive sites are synchronized quite well. As a result, they almost match the cell-averaged calcium concentration. For the wave given in Fig. 1(C), the oscillation period is 7.86 s, which is about 3.8 times of the puff period shown in Fig. 1(A), and the oscillation lifetime is 1.09 s, which is eight times the puff lifetime shown in Fig. 1(A).

Figure 1(D) shows the calcium signals obtained with the Langevin approach. One can see that a large diffusion coefficient generates a strong coupling among the calcium signals at different sites, leading to synchronization of calcium oscillations in the system. The strong coupling also suppresses the channel stochasticity. Therefore, the Ca^{2+} wave with stochastic channel dynamics [Fig. 1(D)] is similar to that with deterministic channel dynamics [Fig. 1(C)]. For this example, the maximal cross correlation between signals at two nearby clusters is about 1.0 [Fig. 2(C)], indicating a quite well synchronization among clusters. Figure 2(B) shows the space-time plots of the waves with stochastic channel dynamics and randomized initial conditions.

Both experiments and simulations suggested that the stochasticity of IP_3R channels plays important role in the initiation of puffs and the onset of waves [5,10,15,19]. In this paper, with the IP_3 concentration set at $[IP_3]=1.0\ \mu M$, the Li-Rinzel point model is set to the oscillatory state, and so the mean lifetime of the stochastic puffs or waves, which is the focus of the paper, will be well described by the deterministic dynamics. Furthermore, the stochastic effects of channel dynamics are not the focus in this paper and we are more interested in the effects of the inhomogeneity of the channel distribution on the calcium dynamics. Thus, we will consider mainly the deterministic channel dynamics in the following discussions.

C. Transition from puff to wave by changing the diffusion coefficient

In a homogeneous active medium, the modification of the diffusion coefficient will typically change the propagation speed of the oscillating waves but should usually not modify the oscillation frequency and signal lifetime. However, one finds that in our inhomogeneous medium, the variation of the diffusion coefficient will change both the oscillation frequency and lifetime.

In Figs. 3(A)–3(C), the calcium signal properties are plotted as a function of D. At small D with $D<2\ \mu m^2/s$, for which one cannot observe global waves [Fig. 3(A)], the puffs show a large oscillation amplitude, which decreases with the increase of D [Fig. 3(B)]. Figure 3(C) shows that the oscillation period of the puff decreases with increasing D at $D<2\ \mu m^2/s$, and the puff lifetime has a slight increase. Once

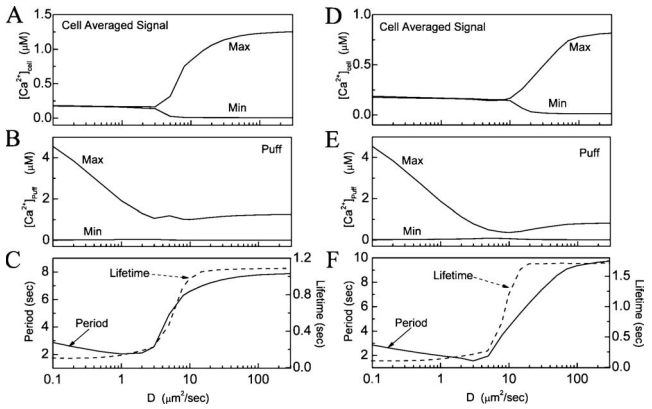

FIG. 3. The Ca^{2+} signals as a function of D at (A)–(C) $L=2$ μm and (D)–(F) $L=3$ μm. In (A) and (D), the maximum and minimum of the cell-averaged signal are plotted; in (B) and (E), the maximum and minimum of the Ca^{2+} puff at the active region of the cell center are plotted; and in (C) and (F), the oscillation period (solid line) and the lifetime (dashed line) of the puff are plotted.

$D>2$ $\mu m^2/s$, a global wave can be observed and the oscillation amplitude of the cell-averaged calcium increases with the increase of D [Fig. 3(A)]. The oscillation amplitude at active regions increases slightly [Fig. 3(B)] and both the period and lifetime increase strongly [Fig. 3(C)].

In Fig. 2(C), the maximal cross correlation between calcium concentrations at the central cluster and its nearby cluster has been calculated as a function of diffusion coefficient. The results show that a weak coupling is found at $D<2$ $\mu m^2/s$, while with $D>10$ $\mu m^2/s$ the clusters couple to each other strongly.

D. Two limits of the Ca^{2+} cell model

In order to discuss how the diffusion coefficient modulates the Ca^{2+} release dynamics (such as oscillation period and lifetime) at active regions, we now consider the two limits of the model, i.e., small and large D.

For small D, each action region can be treated as an independent domain, and its dynamics can be described by

$$\frac{\partial[Ca^{2+}]}{\partial t} = v_C m_\infty^3 n_\infty^3 h^3([Ca^{2+}]_{ER} - [Ca^{2+}]) - v_P \frac{[Ca^{2+}]^2}{k^2 + [Ca^{2+}]^2} + v_L([Ca^{2+}]_{ER} - [Ca^{2+}]) \quad (12)$$

with h's dynamics given in Eq. (8).

However, at a large D, the coupling is so strong that active and passive regions experience almost the same calcium concentration (Fig. 2). As a result, one has $\nabla^2[Ca^{2+}] \to 0$ for the system. In other words, with a large diffusion coefficient, the active regions and passive regions are merged together to become a mixed region. The dynamics for such a mingled state are an average of active and passive regions, which can be described by a point model with

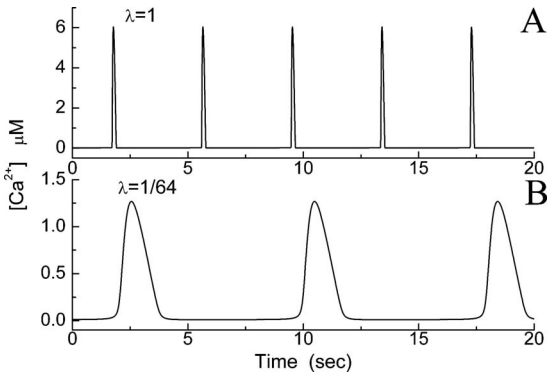

FIG. 4. Oscillations in the point models with (A) Eq. (12) and (B) Eq. (13) with $\lambda=1/64$ at $[IP_3]=1.0$ μM.

$$\frac{\partial[Ca^{2+}]}{\partial t} = \lambda \left\{ v_C m_\infty^3 n_\infty^3 h^3([Ca^{2+}]_{ER} - [Ca^{2+}]) - v_P \frac{[Ca^{2+}]^2}{k^2 + [Ca^{2+}]^2} + v_L([Ca^{2+}]_{ER} - [Ca^{2+}]) \right\}. \quad (13)$$

Compared to Eq. (12), here a rescale factor λ appears given by

$$\lambda = \frac{S_{active}}{S_{active} + S_{passive}} = \frac{l^2}{L^2}, \quad (14)$$

where S_{active} and $S_{passive}$ are the areas of the active and passive regions, respectively. For example, we have $\lambda=1/64$ at $l=0.25$ μm and $L=2$ μm. The rescaling of the maximum flux strength (ν_P, ν_C, and ν_L) for channels, pumps, and leakage takes into account the mixing of active and passive regions.

In Figs. 4(A) and 4(B), the oscillations of solutions of the point models with Eqs. (12) and (13) are plotted at $[IP_3]=1.0$ μM, respectively. For the model with Eq. (12), the oscillation period is 3.88 s and lifetime is 0.115 s, which are the extreme values for puff dynamics given in Fig. 3 (corresponding to $D=0$). For the model with Eq. (13) ($\lambda=1/64$), the oscillation period is 7.93 s and the lifetime is 1.09 s, which is quite similar to the oscillating wave at $D=200$ $\mu m^2/s$ observed in Fig. 2.

E. Rescaling of flux strength in the point model

Thus, the Ca^{2+} release dynamics at active regions for two cases of the model at small or large D can be explained by the point model but with different time scales in Eq. (13). Such a time-scale factor takes into account the coupling strength of the active and the passive regions caused by the Ca^{2+} diffusion coefficient. For the 2D model at small D with weak coupling, we have a corresponding point model at $\lambda=1$; for the 2D model at large D with strong coupling, we have a corresponding point model at $\lambda=1/64$.

For the 2D model with an intermediate diffusion coefficient, the active regions and passive regions are coupled at certain strength. A reasonable guess is that the 2D Ca^{2+} release dynamics with an intermediate D may be described by the point model with the rescale factor in the range of

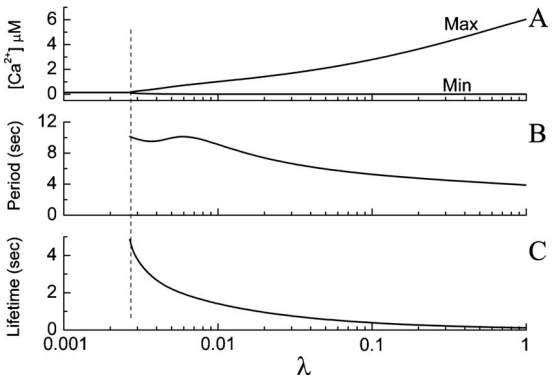

FIG. 5. The solution of the point model [Eq. (13)] as a function of factor λ. (A) The maximum and minimum of $[Ca^{2+}]$, (B) the oscillation period, and (C) the lifetime are plotted. The dotted line marks the bifurcation point.

$1/64<\lambda<1$. Note that the h-gate dynamics [Eq. (8)] do not change with a variation of the diffusion coefficient. We will now check if the point-model approach is valid in the intermediate regime. The point-model dynamics, including the maximum and minimum of calcium concentration, the oscillation period, and the lifetime, as a function of the rescale factor λ are given in Fig. 5.

As a comparison with Fig. 3, it can be seen that for the 2D cell model with the increase of the diffusion coefficient, the oscillation period decreases first and after reaching its minimum around $D=5\ \mu m^2/s$ it increases (Fig. 3). However, the point model does not exhibit such behavior but instead gives a monotonic increasing lifetime with the decrease of the factor λ [Fig. 5(C)]. Thus, the 2D cell model shows complex dynamics at intermediate diffusion coefficient, which cannot be simply discussed with a point model.

F. Modulation of Ca^{2+} wave by the cluster-cluster distance

In the simulations discussed above, the cluster-cluster distance is set to $L=2\ \mu m$. Now we discuss the effect on Ca^{2+} signals of varying the diffusion coefficient at other cluster-cluster distances. Consider an extreme case where the cluster-cluster distance is zero, i.e., $L=l$. In this case, the cellular medium is homogeneously active. Thus, no matter how large or small the diffusion coefficient is, one can always find an oscillating dynamics. This is because at $[IP_3]=1.0\ \mu M$, the related point model is in a spiking state.

In Figs. 3(D)–3(F), the cluster-cluster distance L increases to $3\ \mu m$, but we still keep $l=0.25\ \mu m$. It can be seen that the global wave appears at larger diffusion coefficient if the cluster-cluster distance is larger.

In the following, we focus on global waves at large diffusion coefficient. For large D, the oscillation dynamics can be understood based on the point model of Eqs. (8) and (13) with a rescale factor λ. Equation (14) indicates that the rescale factor λ is a measurement of area ratio between active and passive regions. When keeping $l=0.25\ \mu m$ and letting $L=3\ \mu m$, we obtain $\lambda=1/144$. According to Fig. 5, the oscillation period and lifetime of the point model are then 9.98 and 1.76 s, respectively. For the corresponding 2D cell model, the oscillating Ca^{2+} signal has a period of 9.65 s and lifetime of 1.71 s at $D=200\ \mu m^2/s$ [Fig. 3(F)].

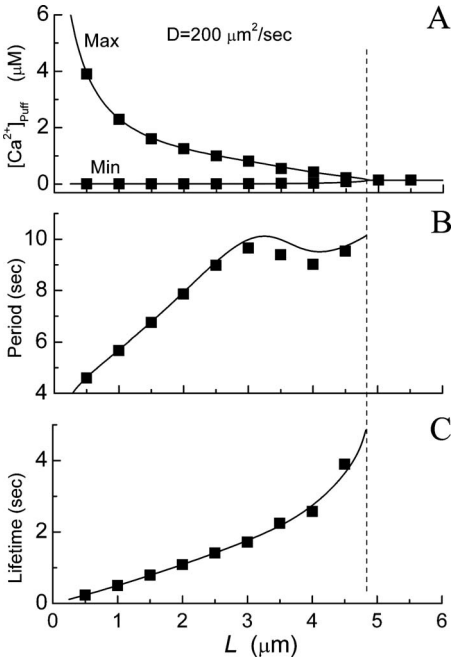

FIG. 6. The oscillation behaviors of the 2D cell model (squares) and the point model (solid line) as a function of L. (A) The maximum and minimum of Ca^{2+} signal, (B) the oscillation period, and (C) the lifetime are plotted. The dotted line marks out the death of global wave.

Figure 5 also shows that fixed points occur at $\lambda>0.0027$ (corresponding to $L>4.83\ \mu m$), indicating that the large cluster distance will destroy the global wave. In Fig. 6, we show the comparison of results of oscillation amplitude, lifetime, and period obtained with the 2D diffusion model at $D=200\ \mu m^2/s$ (squares) and the point model (solid lines) as a function of L. As predicted by the point model, one could not observe the global Ca^{2+} waves at $L>4.83\ \mu m$.

G. Phase diagram

According to the discussion given above, different dynamical regimes in the parameter space of diffusion coefficient D and cluster-cluster distance L can be expected. In detail, puffs are found at small D and large L, while the global waves are typically observed at large D and limited L. At large D, the increase of L will cause the death of oscillations, leading to a fixed point in the cell model.

In order to discuss the phase diagram precisely, now we go back to the two-dimensional model for detailed simulations either with deterministic channel dynamics or with stochastic channel dynamics. The phase diagram obtained with deterministic channel dynamics is given in Fig. 7(A). With deterministic channel dynamics, the death of oscillation can be easily defined as a fixed point in the cell model. However, in the transition region of the phase diagram it is difficult to distinguish the regimes of local puffs and global waves. So we simply define the puff pattern as that the Ca^{2+} oscillation

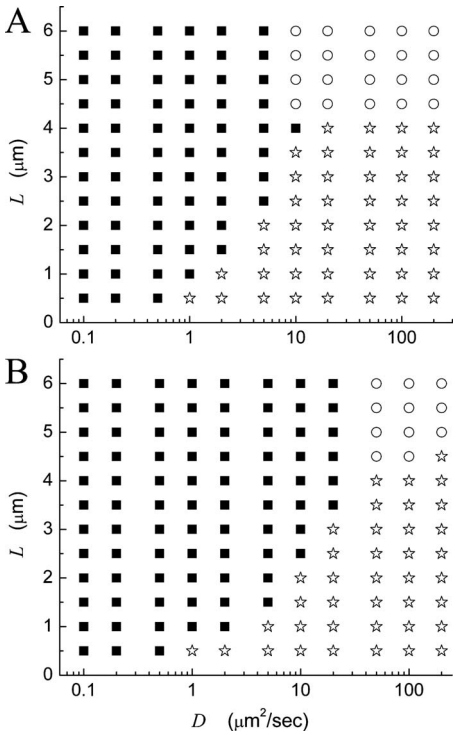

FIG. 7. The phase diagram of the 2D model in terms of diffusion coefficient D and cluster-cluster distance L with (A) deterministic channel dynamics or (B) stochastic channel dynamics at $N=25$ in each cluster. Here, three patterns are distinguished: local puffs (squares), global waves (stars), and death of oscillation with a fixed point in deterministic dynamics or with the Ca^{2+} fluctuation in stochastic dynamics (circles). Here $[IP_3]=1.0\ \mu M$.

amplitude at the cluster site is at least twice of the Ca^{2+} oscillation amplitude at the middle passive site of two nearby cluster sites, otherwise the pattern is defined as the global wave.

With the stochastic channel dynamics, we could not observe the Ca^{2+} pattern with a fixed point. Notice that the typical oscillation amplitudes either for local or global Ca^{2+} signal are typically larger than 1 μM, as shown in Fig. 1 or 3. Thus the death of oscillation is somehow arbitrarily defined as the small fluctuation of Ca^{2+} concentration with the mean oscillation amplitude of cell averaged $[Ca^{2+}]$ smaller than 0.1 μM and the mean oscillation amplitude of $[Ca^{2+}]$ at cluster sites smaller than 0.2 μM. Then we have to distinguish local puffs and global waves. Here two ways are applied to distinguish stochastic puffs from waves. One way which is similar as the method applied for deterministic patterns is to define the puff pattern as that the mean Ca^{2+} oscillation amplitude at the cluster site is at least twice of the mean Ca^{2+} oscillation amplitude at the middle passive site of two nearby cluster sites, otherwise the pattern is defined as the global wave. Another way to distinguish the puffs and waves is to discuss the maximal cross correlation of two Ca^{2+} signals at two nearby clusters. An example is given in Fig. 2(C). If the maximal cross correlation is smaller than 0.5, the pattern is defined as puffs, otherwise, waves. Our simulation results show that both methods produce the same phase diagram, which is given in Fig. 7(B).

IV. DISCUSSION

Experimentally, in large cells, such as *Xenopus laevis* oocytes, a transition between a regime of global oscillations of calcium release and a localized noisy regime has been found [6,7]. This transition can be forced by injection of a slow-binding and slow-diffusing buffer proteins (EGTA) [6]. A noticeable feature of the puff-wave transition is the very short lifetime of puffs (a few hundreds of milliseconds), while global activity is typically present for several seconds. The simulations presented in this paper, with a simple model of spiking elements coupled by diffusion through a passive space, give a possible mechanism accounting for such a lifetime difference.

First, we here assume that EGTA buffer lowers the effective calcium diffusion within the cytosol, thus decoupling the clusters. We found evidence that the decoupling through smaller diffusivity leads to the replication of a puff-wave transition. As shown in Fig. 3 the cell-averaged signal exhibits oscillations for large diffusivity only, while local elements spike for small D. Furthermore, by varying the distance L between the elements, we predicted that for increasing L the transition to waves is shifted toward larger D.

The plots in Fig. 3 also show that for increasing D the lifetime increases from 0.1 to more than 1 s. Thus, our model with two-dimensional diffusion of calcium generates the disparate lifetimes of puffs and waves. The modification of lifetime is then simply explained by the change of time scale of the reaction terms. The increase in lifetime is a unique attribute of the puff-wave transition in calcium signaling, which has evoked different explanations in recent studies [29,30]. Using a more detailed model, Zeller *et al.* [30] found that the competition of EGTA with a simultaneously used dye buffer leads to a faster decay of dye signals after an initial release spike. In a different approach, Rudiger and Schimansky-Geier [29] considered the influence of EGTA on the coupling in arrays of clusters, which they modeled by generic equations for excitable elements. They proposed that coupling of the individual elements can be introduced by a delay-diffusive term in the FitzHugh-Nagumo-type equations for the individual elements. They found that a reduction of coupling strength indeed significantly shortens excitation spikes while large coupling leads to long spikes with large accumulating inhibition.

While the earlier studies attributed the puff-wave transition to either local dye/EGTA dynamics [30] or delay coupling of clusters [29], the transition found in this work is related to the interaction of active elements to the surrounding passive space. This is made apparent by the simplified point model, which captures basic properties of the full system's behavior. The point model assumes that the mixing of the calcium in the simulation domain is strong such that an averaging of passive and active areas becomes possible. Thus the model is valid especially in the case of large diffusivity and can describe the L dependence of oscillation characteristics very well. It could, however, not describe a broader region of interest, which occurs for intermediate values of D.

It has been shown in earlier studies that diffusing calcium builds microdomains around the active clusters with large

local concentration and small concentration between the clusters [30,31]. The difference between the intracluster and intercluster values of calcium concentration depends, of course, on the details of transport processes and leads to the intricate properties of the coupling of clusters discussed in this paper. However, for simplicity, the coupling of channels within the cluster in our model has been assumed to occur through the common value of calcium concentration. This may be a serious limitation of our model since it is not clear if our model includes enough details on the Ca^{2+} transport processes. We expect that future work on detailed models of puffs will clarify this point.

Experimentally the puff-wave transition can also be provoked by varying the level of IP_3 concentration without altering the diffusion coefficient of calcium [5]. It has been suggested that the effective diffusion coefficient of calcium is about 15–35 $\mu m^2/s$ [32]. With the stochastic channel dynamics at this diffusion coefficient, one typically observes, due to the strong couplings [Fig. 2(C)], in the model either the small fluctuation of calcium around its resting state at small IP_3 concentration or global Ca^{2+} waves at large IP_3 concentration and hardly finds the separated puffs. We think that this is possibly due to the approximation of point model assumed for the clustered channels and the approximation of effective diffusion coefficient to account the effect of mobile and immobile buffers. A better realistic Ca^{2+} model is expected to reproduce more experimental observations.

Spatially distributed active systems are widely found in physical, chemical, or biological systems, in which inhomogeneities are ubiquitous. It has been shown that inhomogeneity plays an important role in spatiotemporal dynamics in a number of systems [22,23,33,34]. We finally suggest that our time-rescaled point-model analysis may also be applicable to other inhomogeneous systems.

ACKNOWLEDGMENTS

We thank F. Müller (Berlin) for helpful discussions. J.W.S. would like to acknowledge support of this work by the National Science Foundation of China under Grant No. 10775114 and the National Institutes of Health of USA under Grant No. 2RO1GM065830-06A1.

[1] Y. Yao, J. Choi, and I. Parker, J. Physiol. (London) **482**, 533 (1995).
[2] M. D. Bootman, M. J. Berridge, and P. Lipp, Cell **91**, 367 (1997).
[3] I. Parker and Y. Yao, Proc. R. Soc. London, Ser. B **246**, 269 (1991).
[4] M. J. Berridge, M. D. Bootman, and P. Lipp, Nature (London) **395**, 645 (1998).
[5] X. P. Sun, N. Callamaras, J. S. Marchant, and I. Parker, J. Physiol. (London) **509**, 67 (1998).
[6] S. L. Dargan and I. Parker, J. Physiol. (London) **553**, 775 (2003).
[7] S. L. Dargan, B. Schwaller, and I. Parker, J. Physiol. (London) **556**, 447 (2004).
[8] J. W. Shuai and P. Jung, Biophys. J. **83**, 87 (2002).
[9] J. W. Shuai and P. Jung, Phys. Rev. Lett. **88**, 068102 (2002).
[10] S. Swillens, G. Dupont, L. Combettes, and P. Champeil, Proc. Natl. Acad. Sci. U.S.A. **96**, 13750 (1999).
[11] G. Ullah and P. Jung, Biophys. J. **90**, 3485 (2006).
[12] H. DeRemigio and G. D. Smith, Cell Calcium **38**, 73 (2005).
[13] D. Fraiman, B. Pando, S. Dargan, I. Parker, and S. P. Dawson, Biophys. J. **90**, 3897 (2006).
[14] L. Diambra and N. Guisoni, Cell Calcium **37**, 321 (2005).
[15] J. W. Shuai and P. Jung, Proc. Natl. Acad. Sci. U.S.A. **100**, 506 (2003).
[16] J. W. Shuai and P. Jung, Phys. Rev. E **67**, 031905 (2003).
[17] M. Falcke, Biophys. J. **84**, 42 (2003).
[18] M. Falcke, L. Tsimring, and H. Levine, Phys. Rev. E **62**, 2636 (2000).
[19] A. Skupin, H. Kettenmann, U. Winkler, M. Wartenberg, H. Sauer, S. C. Tovey, C. W. Taylor, and M. Falcke, Biophys. J. **94**, 2404 (2008).
[20] H. DeRemigio, M. D. LaMar, P. Kemper, and G. D. Smith, Phys. Biol. **5**, 036003 (2008).
[21] S. Means, A. J. Smith, J. Shepherd, J. Shadid, J. Fowler, R. J. H. Wojcikiewicz, T. Mazel, G. D. Smith, and B. S. Wilson, Biophys. J. **91**, 537 (2006).
[22] S. P. Dawson, J. Keizer, and J. E. Pearson, Proc. Natl. Acad. Sci. U.S.A. **96**, 6060 (1999).
[23] B. Pando, J. E. Pearson, and S. P. Dawson, Phys. Rev. Lett. **91**, 258101 (2003).
[24] G. D. Smith, J. Wagner, and J. Keizer, Biophys. J. **70**, 2527 (1996).
[25] G. W. De Young and J. Keizer, Proc. Natl. Acad. Sci. U.S.A. **89**, 9895 (1992).
[26] Y. X. Li and J. Rinzel, J. Theor. Biol. **166**, 461 (1994).
[27] N. Callamaras and I. Parker, EMBO J. **19**, 3608 (2000).
[28] J. W. Shuai, H. J. Rose, and I. Parker, Biophys. J. **91**, 4033 (2006).
[29] S. Rudiger and L. Schimansky-Geier, J. Theor. Biol. **259**, 96 (2009).
[30] S. Zeller, S. Rudiger, H. Engel, J. Sneyd, G. Warnecke, I. Parker, and M. Falcke, Biophys. J. **97**, 992 (2009).
[31] R. Thul and M. Falcke, Phys. Rev. Lett. **93**, 188103 (2004).
[32] N. L. Albritton, T. Meyer, and L. Streyer, Science **258**, 1812 (1992).
[33] A. P. Munuzuri, V. Perez-Munuzuri, and V. Perez-Villar, Phys. Rev. E **58**, R2689 (1998).
[34] B. W. Li, H. Zhang, H. P. Ying, and G. Hu, Phys. Rev. E **79**, 026220 (2009).